

Characterization of Two Partially Unfolded Intermediates of the Molecular Chaperone DnaK at Low pH[†]

Michael G. Sehorn, Sergey V. Slepnev, and Stephan N. Witt*

Department of Biochemistry and Molecular Biology, Louisiana State University Health Sciences Center, 1501 Kings Highway, Shreveport, Louisiana 71130-3932

Received March 14, 2002; Revised Manuscript Received April 23, 2002

ABSTRACT: In this study, the effect of pH on the conformation and the reactivity of the *Escherichia coli* Hsp70 molecular chaperone DnaK was investigated using spectroscopic and chemical assays. DnaK exhibits negligible binding of the hydrophobic dye 1-anilino-naphthalene-8-sulfonate (ANS) between pH 7 to 5.0, whereas appreciable binding occurs between pH 4.5 to 4.0. The binding of ANS to a protein is diagnostic of the presence of accessible ordered hydrophobic surfaces. Such hydrophobic surfaces are often displayed by partially folded protein intermediates such as molten globules. Nucleotide inhibits 70% of the ANS binding at pH 4.5 but none of the ANS binding at pH 4.0. Proteolysis of nucleotide-free DnaK at pH 4.5 with cathepsin D yields detectable fragments (masses > 20 kDa) of the C-terminal peptide-binding domain but none of the N-terminal ATPase domain, thus the ATPase domain is preferentially targeted for proteolysis. In contrast, proteolysis of nucleotide-free DnaK at pH 4.0 with cathepsin D cuts near the linker region, yielding both functional domains. Our interpretation of these data is that incubation of DnaK at pH 4.5 produces a partially unfolded form of the ATPase domain, in which secondary structure is mainly intact, but tertiary structure is reduced. Incubation of the protein at pH 4.0 produces an intermediate in which both functional domains have collapsed and possibly separated. Nucleotide inhibits the conformational change that occurs at pH 4.5 but not at 4.0.

The Hsp70 molecular chaperone DnaK plays an essential role in *Escherichia coli* by mediating the folding, transport, and assembly of other proteins in an ATP-dependent activity cycle (1–4). DnaK, together with its co-chaperones (DnaJ and GrpE), functions co-translationally to stabilize nascent chains in cooperation with the protein trigger factor, which is a prolyl isomerase (5, 6). DnaK and its co-chaperones also function posttranslationally to disaggregate proteins in cooperation with ClpB (7–9). Nascent or heat-inactivated proteins exhibit partially unfolded segments of polypeptide chain to which DnaK selectively binds. Through repeated cycles of substrate binding and release, DnaK facilitates, by an unknown mechanism, the folding or renaturation of substrate proteins.

DnaK is composed of two functional domains: the N-terminal ATPase domain and the C-terminal peptide-binding domain are composed of residues 1–388 and 389–638, respectively. The ATPase domain is a bilobed structure that contains a deep channel between the two lobes (Figure 1A) (10, 11); nucleotide binds at the base of the channel. The polypeptide-binding domain consists of a uniquely folded β -sandwich subdomain followed by an α -helical subdomain composed of five α -helices (Figure 1B) (12, 13). This α -helical subdomain is like a lid over the β -sandwich subdomain (13). Like a latch, a network of hydrogen bonds and a salt bridge links the lid noncovalently to the β -sand-

wich. A peptide molecule binds to the β -sandwich but does not interact with the lid.

The unique interplay between the two functional domains of DnaK creates a ligand-activated, bidirectional molecular switch. As examples, ATP binding to the ATPase domain induces a conformational change that is rapidly propagated to the C-terminal domain (14–17), and this results in a $\sim 10^4$ -fold acceleration in the rate of peptide dissociation from the peptide-binding domain. Conversely, peptide binding to the C-terminal domain of ATP-bound DnaK induces a conformational change that is propagated to the ATPase domain (14), and this results in a stimulation of the rate of ATP hydrolysis. Unfortunately, the lack of a crystal structure for an intact Hsp70 chaperone has prevented a detailed understanding of the structural basis for the coupling between the two domains.

Insights into domain–domain interactions in DnaK have come about from studying the denaturation of DnaK by heat and chemical denaturants (18–20). Denaturation studies of multidomain proteins such as DnaK are of general interest because they offer insights into how separate folding units influence one another. These studies on DnaK are possible because DnaK, unlike its eukaryotic counterparts, exhibits reversible thermal- and chemical-induced unfolding. Montgomery and colleagues (19) showed using differential scanning calorimetry that nucleotide-free DnaK unfolds in three discrete transitions, centered at 45.2, 58.0, and 73.3 °C at pH 7.6, which is consistent with a minimum of four states of DnaK on its unfolding pathway. The three transitions were proposed to arise from two independent coopera-

[†] Support for this work came from the NIH (GM51521).

* To whom correspondence should be addressed. Tel: (318) 675-7891. FAX: (318) 675-5180. E-Mail: switt1@lsuhsc.edu.

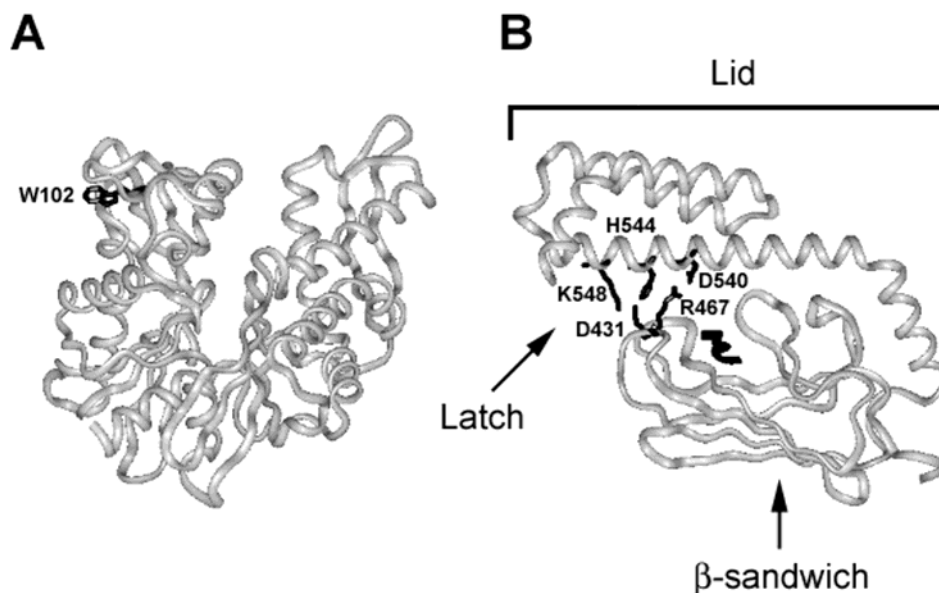


FIGURE 1: (A) Structure of the N-terminal ATPase domain of DnaK (11). DnaK contains only one tryptophan residue, located at position 102. The image was created using the Brookhaven image file 1DKG. The sole tryptophan residue in DnaK, Trp¹⁰², is shown in black. (B) Structure of the C-terminal polypeptide-binding domain of DnaK (13). The NR peptide (NRLLLLTG) is bound in the peptide-binding site. The key amino acids that latch the lid to the β -sandwich are indicated. The image was created using the Brookhaven image file 1DKX.

tive folding units in the N-terminus (N1 and N2) and three independent cooperative folding units in the C-terminus (C1a, C1b, and C2). The low, intermediate, and high temperature transitions were assigned to the N1, C1a, and C1b, and the N2 and C2 cooperative folding units, respectively. The number of folding units in a protein is not necessarily the same as the number of functional domains. The results from this study are consistent with a hierarchical mechanism of folding in which the folding units of DnaK fold or unfold sequentially.

Although partially unfolded intermediates produced upon heating have not been isolated and characterized, a stable compact intermediate of DnaK has been shown to form upon incubation of the protein at relatively low concentrations of guanidine hydrochloride (Gdn·HCl) (20). This intermediate has been characterized in detail. Specifically, between 0.3 and 1.6 M guanidine hydrochloride the Stokes radius of DnaK expands monotonically by 35% compared to the native protein, and the hydrophobic dye bis-ANS¹ binds to the expandable intermediate, whereas no appreciable dye binding occurs in the absence of denaturant. Such results are consistent with the formation of an intermediate in which tertiary structure is reduced, while secondary structure is mostly intact. The hydrophobic core of this intermediate is accessible and thus readily binds bis-ANS.

In a related study, domain–domain interactions in the two-domain protein rhodanese were investigated using bis-ANS to probe hydrophobic surfaces in conjunction with digestion by trypsin at pH 7 (21). Incubation of rhodanese with up to 3 M urea has little effect on its activity, whereas incubation at 4.25 M leads to a time-dependent loss of the activity. Bis-

ANS fluorescence is intense in the presence of rhodanese and 4.25 M urea but negligible at 0, 3, or 6 M urea. Interestingly, tryptic digestion of rhodanese in the presence of 4.25 M urea yields the two domains. It was concluded that this concentration of urea induces domain separation and concomitant exposure of a linker region between the two domains. Hence, domain separation precedes the global unfolding of rhodanese.

In this study, we examined the effect of pH on the conformation and reactivity of the molecular chaperone DnaK. We were interested in characterizing stable partially unfolded forms of DnaK as a way to probe domain–domain interactions and also in examining how pH affects DnaK's ability to hydrolyze ATP and bind peptide. Evidence for the formation of two stable intermediates of DnaK is presented. The role of nucleotide in stabilizing the conformations of these intermediates is discussed.

MATERIALS & METHODS

Reagents. All reagents were purchased from Sigma Chemicals, unless otherwise noted. DnaK was purified as described (22, 23) and maintained in 25 mM *N*-(2-hydroxyethyl) piperazine-*N'*-2-ethanesulfonic acid (HEPES)/50 mM KCl/5 mM MgCl₂/5 mM 2-mercaptoethanol at pH = 7.0. An additional purification step was carried out for DnaK that was used in the proteolysis assay (see "Protease digestion of DnaK" below). SDS–PAGE analysis demonstrated that the DnaK preparations were $\geq 95\%$ pure. Protein concentration was determined using a BioRad protein assay kit according to the manufacturer's instructions. Nucleotide-free DnaK was prepared either by an exhaustive 4-day dialysis or using the chemical method of Gao (24–26). No differences were found between nucleotide-free protein prepared by these two methods.

Peptides were synthesized by Genemed Synthesis Incorporated (S. San Francisco, CA), purified to $>95\%$ by HPLC, and the mass verified by electrospray mass spectroscopy.

¹ Abbreviations: bis-ANS, 1,1'-bis(4-anilino-5-naphthalenesulfonic acid); ANS, 1-anilino-naphthalene-8-sulfonate; fCro, α -*N*-dansyl-MQQRITLKNYAM; fNR, α -*N*-dansyl-NR peptide; fp5, α -*N*-dansyl-CLLSAPRR; Gdn·HCl, guanidine hydrochloride; HEPES, *N*-(2-hydroxyethyl) piperazine-*N'*-2-ethanesulfonic acid; HPLC, high-performance liquid chromatography; MES, 2-(*N*-morpholino) ethanesulfonic acid.

The NR (27) and p5 peptides (28) were dansylated at their N-termini and purified as described (29) (fNR, α -N-dansyl-NRLTLTG; fp5, α -N-dansyl-CLLLSAPRR). A Cro peptide analogue was also used. This peptide was labeled at its N-terminus and purified as described (fCro, α -N-dansyl-MQQRITLKNYAM) (22).

ATPase Assay. The steady-state rate of DnaK-mediated ATP hydrolysis (k_{cat} [mol of ATP (mol of DnaK) $^{-1}$ min $^{-1}$]) was measured by separating [2,8- ^3H]ATP from [2,8- ^3H]ADP using PEI cellulose plates as previously described (22) with minor modifications. Samples were prepared (3–14 μM DnaK; 0 – 600 μM peptide; 10 μM [2,8- ^3H]ATP (36 Ci/mmol) (NEN, 1 Ci = 3.7×10^{10} Bq); and 70 μM ATP) and then the pH was shifted to the desired pH by mixing with an equal volume of a pH-adjusting buffer (see “pH Jumps” below). Reactions conducted at pH ≤ 4.5 were composed of the following reagents (60 μL): 3–14 μM DnaK; 10, 30, or 50 μM [2,8- ^3H]ATP (36 Ci/mmol) (NEN, 1 Ci = 3.7×10^{10} Bq); and 70, 180, or 350 μM ATP; 0 – 600 μM peptide; and 20 mM Mg^{2+} . Reported steady-state turnover numbers, obtained at saturating conditions of ATP, peptide, and Mg^{2+} , represent the difference between DnaK-catalyzed and uncatalyzed ATP hydrolysis.

Because several experiments were conducted in the presence of ATP at 35 $^{\circ}\text{C}$ (5 μM DnaK, 1 mM ATP), an obvious question is how much ATP was hydrolyzed by DnaK over the course of 10–20 min at 35 $^{\circ}\text{C}$. If significant amounts of ADP were produced, then samples containing ATP could also contain ADP–DnaK complexes. To estimate how much ADP was produced during incubation at 35 $^{\circ}\text{C}$, measured values for k_{cat} (25 $^{\circ}\text{C}$) (3.8×10^{-2} min $^{-1}$ at pH 4.5; 3.6×10^{-2} min $^{-1}$ at pH 7.0, and 6.9×10^{-2} min $^{-1}$ at pH 9.0) were extrapolated to 35 $^{\circ}\text{C}$ using the relation

$$k_{\text{cat}}(35^{\circ}\text{C}) = k_{\text{cat}}(25^{\circ}\text{C}) \exp\left[\frac{-\Delta H^*}{R}\left(\frac{1}{T_1} - \frac{1}{T_2}\right)\right] \quad (1)$$

The ΔH^* value of 25.0 kcal/mol, obtained at pH 7.0 (25), was used to estimate k_{hy} values at pH 4.5 and 9.0; $T_1 = 308$ K and $T_2 = 298$ K; and $R = 1.987 \times 10^{-3}$ kcal mol $^{-1}$ K $^{-1}$. The above relation yielded k_{cat} (35 $^{\circ}\text{C}$) values of 0.148 min $^{-1}$ (pH 4.5), 0.142 min $^{-1}$ (pH 7.0), and 0.272 min $^{-1}$ (pH 9.0). Using these k_{cat} values we estimate that 15, 15, and 27 μM ADP was produced at pH 4.5, 7.0, and 9.0, respectively, after a 20 min incubation at 35 $^{\circ}\text{C}$. Under the conditions where there is a large excess of ATP over ADP, the occupation of DnaK with ATP is given by

$$\frac{[\text{DnaK} \cdot \text{ATP}]}{[\text{DnaK}]_{\text{tot}}} = \frac{k_{\text{off}}^{\text{ADP}}}{k_{\text{off}}^{\text{ADP}} + k_{\text{cat}}} \quad (2)$$

where $k_{\text{off}}^{\text{ADP}}$ is the rate constant for the dissociation of ADP from DnaK. At pH 7.0 and 35 $^{\circ}\text{C}$, $k_{\text{off}}^{\text{ADP}} = 0.038$ s $^{-1}$ (25) and $k_{\text{cat}} = 2.4 \times 10^{-3}$ s $^{-1}$, and thus 94% of the DnaK molecules are bound with ATP and 6% with ADP. If $k_{\text{off}}^{\text{ADP}}$ changes in a comparable way to k_{cat} as the pH is varied, it is expected that $[\text{DnaK} \cdot \text{ATP}] \gg [\text{DnaK} \cdot \text{ADP}]$.

Fluorescence Measurements. A Photon Technology Inc. StrobeMaster pulsed lamp fluorescence lifetime spectrometer with a SE-900 steady-state fluorescence option (So. Brunswick, NJ) was used to obtain lifetime and steady-state data.

For each type of measurement, samples were maintained in a quartz cuvette (1-cm path length) with constant stirring and temperature control via an external circulating heating/cooling bath ($\Delta T = \pm 0.2$ $^{\circ}\text{C}$). The spectrometer was equipped with a N $_2$ flash lamp and gated photomultiplier tube. DnaK samples were excited at 295 nm, and the time-resolved emission decay was collected at 350 nm. For each sample, the lifetime was determined at 10, 30, 60, 90, and 150 min after the pH jump. In almost all cases, the fluorescence decays were best fit by a double-exponential function. The average lifetime, τ_{ave} , reported herein was calculated according to

$$\tau_{\text{ave}} = [\alpha_1(\tau_1)^2 + \alpha_2(\tau_2)^2]/[\alpha_1\tau_1 + \alpha_2\tau_2] \quad (3)$$

where $\alpha_{1,2}$ and $\tau_{1,2}$ are the amplitudes and lifetimes (30), respectively. τ_{ave} had no appreciable dependence on wavelength over the range of 320–360 nm. Lifetime measurements, made on different preparations of DnaK, had associated errors of approximately ± 0.2 – 0.3 ns.

Circular Dichroism (CD). Spectra were recorded on an Olis DSM 16 CD spectrophotometer using a 1-mm path quartz cell. The spectral bandwidth was 2 nm, and data were collected between 200 and 260 nm with 1 datum/2 nm. A variable time constant was used in which the magnitude of the time constant varied inversely with the signal voltage. Spectra were constructed from the average of five scans of the sample minus the average of five scans of the buffer blank. Concentrations after mixing were 2.5 μM DnaK, 500 μM nucleotide, and 100 μM dithiothreitol. Samples were preincubated at 35 $^{\circ}\text{C}$ for 60 min (nucleotide-free and ATP-bound DnaK) or 10 min (ATP-bound DnaK) before spectra were recorded. Mean residue ellipticity, $[\Theta]$, was calculated according to Adler et al. (31).

High-Performance Size Exclusion Chromatography (HPSEC). A Toso-Haas size-exclusion column (G3000SW; 7.5×600 mm) and guard column (TSK-SW; 7.5×75 mm) were connected to a Gilson two-pump HPLC system (22). The mobile phase was the HEPES sample buffer. The flow rate was 1 mL/min. The column and buffers were maintained at room temperature. DnaK (10 μM), fluorescent peptide (10 μM), and nucleotide (1 mM) were incubated for 15 min at 35 $^{\circ}\text{C}$ prior to injection. The DnaK–fNR complex and free fNR peptide eluted at 15.3 and 24.5 mL, respectively. The percent of DnaK bound with the fNR peptide was calculated by integrating the peaks due to DnaK–fNR and fNR, respectively, in the 335 nm absorbance-detected chromatogram. Specificity controls showed that the binding of the fNR peptide to DnaK at pH 4.5, 7.0, and 9.0 was competitively inhibited by excess unlabeled NR peptide. A control was also conducted to make sure that the small but reproducible amount of ADP–DnaK–fNR complex formation at pH 4.5 was not actually due to rapid complex formation on the column. When DnaK, fluorescent peptide, and ADP were mixed on ice at pH 4.5 and immediately injected on to the high performance sizing column (where a rapid shift to pH 7 occurred), there was no detectable DnaK–fluorescent peptide complex formation. This control ruled out that rapid complex formation occurred on the column.

Protease Digestion of DnaK. DnaK purified as described above was subjected to an additional purification step prior

to being digested with protease. Approximately 1 mg of DnaK containing 1 mM ATP was injected onto the Toso-Haas size-exclusion column (G3000SW; 7.5 × 600 mm), and the DnaK monomer peak was collected. Nucleotide was then removed as described above. Cathepsin D was purchased from Athens Research & Technology (Athens, GA). Digestions were conducted as follows: 125 μ L of 20 μ M DnaK with or without 2 mM nucleotide in the HEPES sample buffer was mixed with 125 μ L of the appropriate pH-adjusting buffer (see below); the resultant pH was either 4.5 or 4.0. The sample was then placed in a 35 °C water bath, and after 10 min cathepsin D (1 μ L of 0.3 U/ μ L) was added. Aliquots (25 μ L) were periodically removed, and the digestion was halted by boiling the sample for 3 min in the presence of gel loading buffer (10 μ L). Samples were analyzed using 12.5% Laemmli gels (32). A total of 1.5 μ g of protein was loaded per well. Gels were stained with silver following Morrissey et al. (33).

Some cathepsin D fragments of DnaK were subjected to N-terminal sequencing. A DnaK digest (14 μ g) was run on a 12.5% Laemmli gel and then electroblotted to an Immobilon-P^{8Q} polyvinylidene fluoride membrane (Millipore). Bands were excised, and the protein therein was subjected to N-terminal amino acid sequencing at the Macromolecular Structure Analysis Facility, University of Kentucky, Lexington. Fragments were subjected to five Edman degradation cycles.

Some of the cathepsin D fragments of DnaK were also analyzed by mass spectrometry to determine their precise mass. DnaK was proteolyzed with cathepsin D as described above and then subjected to reversed-phase high performance liquid chromatography to separate fragments. A Vydac C-4 column, equilibrated in water with 0.1% trifluoroacetic acid (eluent A), was connected to a two pump Gilson high-performance liquid chromatography system. A linear AB gradient (2% B/min), where eluent B was 99.9% acetonitrile with 0.1% trifluoroacetic acid, at 1.0 mL/min separated the DnaK fragments. Lyophilized, purified fragments of DnaK were resuspended in 0.1% TFA and analyzed by matrix assisted laser desorption ionization time-of-flight mass spectroscopy (LSU Health Sciences Center, Shreveport, LA). Purified fragments were also subjected to SDS-PAGE.

pH Jumps. pH jumps were achieved by mixing DnaK (in the 25 mM HEPES sample buffer, pH 7.0) with an equal volume of the pH-adjusting buffer. Buffers with no appreciable binding to Mg²⁺ were chosen (34). The salts of each of the adjusting buffers were dissolved in a solution of 50 mM KCl, 25 mM HEPES, 5 mM MgCl₂, and 5 mM 2-mercaptoethanol. Potassium acetate (0.2 M) buffers were used for pH 4.0, 4.5, and 5.0. 2-(*N*-morpholino)ethanesulfonic acid (MES) (0.2 M) buffers were used for pH 5.5, 6.0, and 6.5. HEPES (0.2 M) buffers were used at pH 7.0 and 8.0. Glycine-KOH (0.2 M) buffers were used for pH 9.1 and 10.4. Neat acetic acid was used to adjust the pH of the acetate buffers, whereas a concentrated solution of potassium hydroxide was used to adjust the pH of the MES, HEPES, and glycine buffers. Upon mixing any one of the above buffers with an equal volume of a solution of DnaK, the resultant pH was within 0.1 pH unit of the pH of the adjusting buffer.

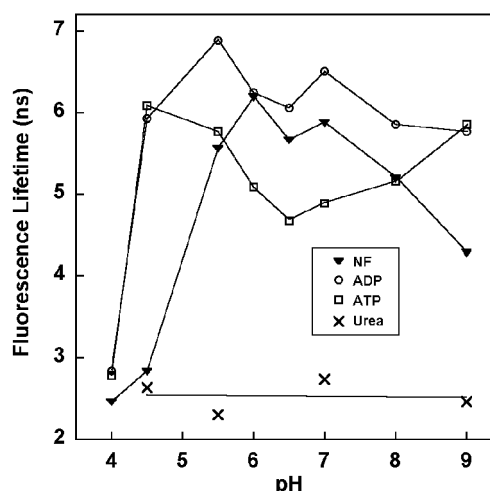


FIGURE 2: pH-dependence of Trp¹⁰² fluorescence lifetime. ▼, nucleotide-free (NF); ○, + ADP; □, + ATP; and ×, 8 M urea. τ_{ave} values were obtained after 60 min of incubation for nucleotide-free and ADP-bound DnaK and after 10 min of incubation for ATP-bound DnaK. Conditions: temperature = 35.0 °C, 5 μ M DnaK, 1 mM ADP or ATP, 8 M urea; λ_{ex} = 295 nm and λ_{em} = 350 nm, respectively. The solid lines are to guide the eye.

RESULTS

The fluorescent amino acid tryptophan is a reporter group for monitoring conformational changes in proteins (35). Because DnaK possesses only one tryptophan residue (Trp¹⁰²), located on the outside portion of the cleft between the two main lobes of the ATPase domain (Figure 1A), changes in tryptophan fluorescence indicate changes in the conformation of the ATPase domain. It is well-known that ATP binding rather than hydrolysis induces a conformational change in both domains of DnaK (15, 17), resulting in both a 15% reduction and a blue-shift of DnaK's tryptophan fluorescence (18, 36). Lodged in the cleft between the two lobes, a bound nucleotide molecule does not directly contact Trp¹⁰².

pH-Induced Conformational Changes in the N-Terminal Domain of DnaK. In this section, we initially investigated the susceptibility of the ATPase domain of DnaK to acid- and base-induced conformational changes by measuring the average fluorescence lifetime (τ_{ave}) of Trp¹⁰² as a function of pH. Plots of τ_{ave} for nucleotide-free, ADP-, ATP-bound, and urea-denatured DnaK as a function of pH are shown in Figure 2. DnaK denatured with urea exhibits a 2.6 ns tryptophan lifetime over the pH range 3–10. Focusing on the low pH side of the plots, τ_{ave} = 6.0 ± 0.1 ns for nucleotide-bound DnaK (ADP or ATP) at pH 4.5, whereas τ_{ave} = 2.8 ns for nucleotide-free DnaK, which is almost the same as that for urea-denatured DnaK. At pH 4.0, τ_{ave} is much less sensitive to the presence of nucleotide (τ_{ave} = 2.5–2.8 ns). The data show that nucleotide protects the ATPase domain of DnaK at pH 4.5 but not at pH 4.0 against an acid-induced conformational change, possibly unfolding, that quenches the fluorescence of Trp¹⁰².

Far-UV Circular Dichroism. To ascertain the extent of DnaK unfolding at low pH, the secondary structure of DnaK was probed using far-UV circular dichroism (Figure 3 A–D). Spectra of the various states of DnaK (NF, ADP- or ATP-bound) are compared to the spectrum of urea-denatured DnaK. Similarities and differences in the spectra are sum-

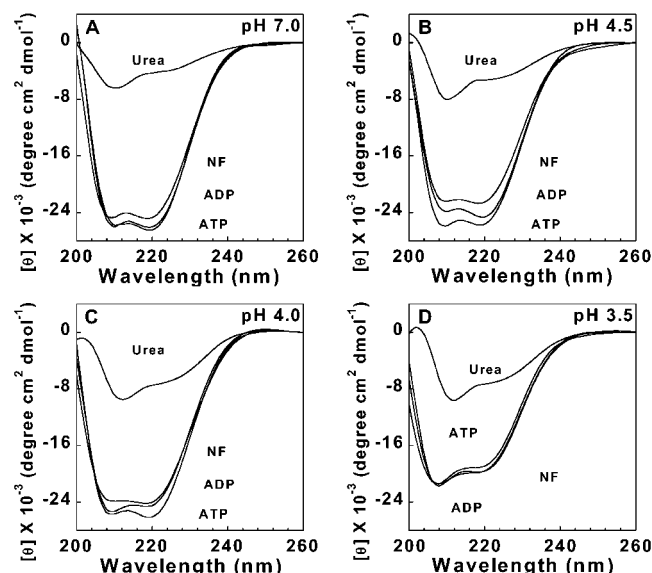


FIGURE 3: Far-UV circular dichroism spectra of DnaK. (A) pH 7.0; (B) pH 4.5; (C) pH 4.0; (D) pH 3.5. Spectra were recorded after a 10 min preincubation of the sample at 35 °C. Conditions: 2.5 μ M DnaK, 0.5 mM ADP, 0.5 mM ATP, or 7.0 M urea; temperature = 35 °C. Each spectrum represents sample minus buffer blank. NF indicates nucleotide-free DnaK.

marized as follows. (i) The CD spectra of DnaK acquired at pH 7.0, 4.5, and 4.0 all show negative peaks at 208 and 220 nm (Figure 3A–C), which is consistent with significant amounts of α -helical structure. In contrast, the CD spectra of DnaK acquired at pH 3.5 (Figure 3D) exhibit a prominent negative peak at 208 nm. (ii) The CD spectra of DnaK collected between pH 7.0–4.0 and at pH 3.5 are sensitive and insensitive to the presence of nucleotide, respectively. (iii) Because the CD spectra of nucleotide-free, ADP-, and ATP-bound protein are not superimposable on the spectrum of urea-denatured DnaK at pH 3.5, DnaK must retain a significant amount of secondary structure at this pH. These experiments show that at pH 4.5 or 4.0, whether nucleotide-free or nucleotide-bound, the secondary structure content of DnaK is similar to that of the protein at pH 7. The results are interpreted to mean that nucleotide-free DnaK is not unfolded at pH 4.5 or 4.0. The relatively short Trp¹⁰² fluorescence lifetime in the nucleotide-free protein at pH 4.5–4.0 may result from quenching due to protonation of a nearby residue (Figure 2).

Exposed Hydrophobic Surfaces Probed by ANS Binding. It is well-known that upon lowering the pH to 4.5–4 many proteins convert to an A-state (37). An A-state is a compact intermediate in which tertiary structure is reduced or eliminated while secondary structure is mainly intact, similar to the native state. One of the defining features of an A-state is that its hydrophobic core is relatively accessible and readily binds the environmentally sensitive dye 1-anilino-naphthalene-8-sulfonate (ANS). When a protein is incubated with ANS at low pH, increases in ANS fluorescence are diagnostic of the presence of accessible ordered hydrophobic surfaces (38).

ANS binding experiments were conducted to test the hypothesis that nucleotide-free DnaK adopts a conformation with accessible ordered hydrophobic surfaces at low pH. A plot of ANS fluorescence at 485 nm versus pH is shown in Figure 4. In each experiment, DnaK was incubated with 25

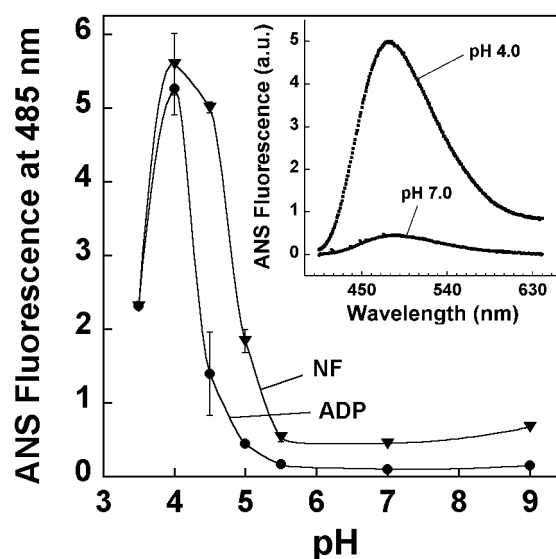


FIGURE 4: pH dependence of ANS fluorescence intensity in the presence of DnaK. ANS fluorescence at 485 nm is plotted for nucleotide-free DnaK (●) and ADP-DnaK (▼). Conditions: temperature = 35.0 °C; 1 μ M DnaK, 1 mM ADP, and 25 μ M ANS, and λ_{ex} = 354 nm. Excitation and emission slits were 2 and 5 nm, respectively. Inset, fluorescence difference spectra [(ANS + nucleotide-free DnaK) – ANS] at the indicated pH. Spectra were recorded after a 60 min incubation of the dye with the protein at the indicated pH. NF indicates nucleotide-free DnaK.

μ M ANS at the indicated pH at 35 °C in the presence or absence of ADP, and after 60 min the fluorescence spectrum of ANS was recorded. For experiments conducted using nucleotide-free DnaK, the plot of ANS fluorescence versus pH shows negligible ANS binding to DnaK over the pH range 5.5 to 9.0, whereas a bell-shaped region of intense ANS binding occurs at low pH, centered at pH 4.0 and with inflection points at pH 4.8 and 3.8. A similar profile occurs for ANS binding to ADP-bound DnaK, that is, negligible ANS binding to DnaK occurs over the pH range 5.0 to 9.0 but a narrower bell-shaped region of intense ANS binding occurs at low pH, centered at pH 4.0 and with inflection points at pH 4.3 and pH 3.8. The inset shows ANS fluorescence spectra for samples of ANS mixed with nucleotide-free DnaK and incubated at pH 7.0 or pH 4.0. These data are interpreted to mean that DnaK exhibits accessible ordered hydrophobic surfaces at pH 4.5 and pH 4.0 that are not present at pH 7.0. ADP binding prevents the display of these hydrophobic surfaces at pH 4.5 but not at pH 4. The possibility that DnaK converts to an A-state at these low pHs is discussed below.

ATPase Activity Assay. Experiments were conducted to determine whether the intermediates of DnaK produced at low pH mediate ATP hydrolysis. Figure 5 A shows the steady-state ATPase activity (k_{cat}) of DnaK as a function of pH at 25 °C. A saturating concentration of NR peptide results in a 5- and 2-fold increase in the ATPase activity of DnaK at pH 7.0 and 9.0, respectively; however, the NR peptide even up to 600 μ M has no effect on the ATPase activity at pH 4.5. No detectable DnaK-mediated ATP hydrolysis occurs at pH < 4.5, even at very high concentrations of ATP, Mg^{2+} , and NR peptide. Notice that the loss of steady-state ATPase activity exactly parallels the decrease in fluorescence lifetime as the pH is lowered from 4.5 to 4.0 (Figure 2).

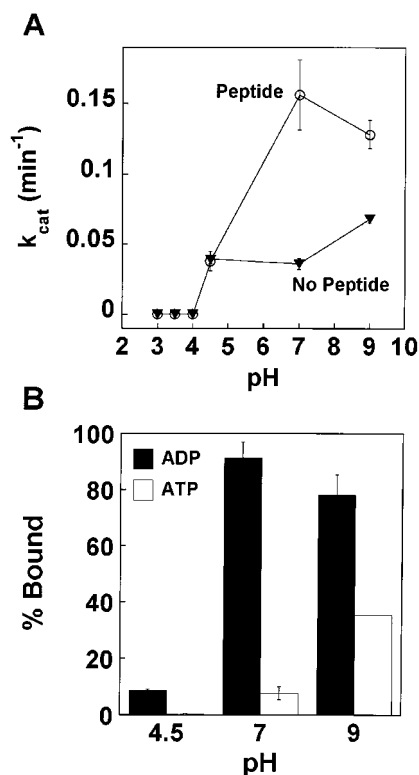


FIGURE 5: pH-dependence of DnaK's ATPase and peptide binding activities. (A) Plot of steady-state ATPase activity of DnaK (k_{cat}) versus pH. Reported k_{cat} values are for saturating conditions of ATP, Mg^{2+} , and peptide. Conditions: 14.2 μM DnaK (pH 3.0); 5.0, 7.0 μM DnaK (pH 4.5); 2.4, 3.6 μM DnaK (pH 7); and 3.6 μM DnaK (pH 9); temperature = 25 °C. Over the pH range of 4.5–9, the turnover number obtained with 200 μM NR peptide was the same as obtained with 600 μM . (B) Plot of percent DnaK–fNR complex formation versus pH. Samples were incubated for 15 min and then injected onto the sizing column. Conditions: 2 μM DnaK, 1 mM nucleotide, 10 μM fNR; temperature = 35 °C.

Peptide Binding at Low pH. The failure of the NR peptide to stimulate the ATPase activity of DnaK at pH 4.5 may be due to low affinity binding of the peptide to DnaK at this pH. Alternatively, the NR peptide may bind to DnaK with high affinity, but interdomain coupling is disrupted. To distinguish between these two possibilities, the amount of DnaK–fNR complex formation as a function of pH was determined using high performance size exclusion chromatography (Figure 5B). The amount of peptide binding to DnaK under equilibrium conditions was measured at pH 9, 7, and 4.5. DnaK (2 μM), the fNR (10 μM) peptide, and nucleotide (1 mM ADP or ATP) were incubated at 35 °C for 15 min and then an aliquot was injected on the sizing column maintained at room temperature. At pH 7.0, as expected, the fNR peptide binds tightly to ADP–DnaK, and the amount of peptide binding is significantly reduced when ATP is substituted for ADP. Similar results were obtained at pH 9.0, although ATP was much less effective in reducing the amount of DnaK–fNR complexes at pH 9.0 than at pH 7.0. Approximately 10% of ADP–DnaK molecules are bound with the fNR peptide at pH 4.5. No detectable complex formation occurs at pH 4.5 when ATP rather than ADP is used. These results are consistent with the hypothesis that the failure of the NR peptide to stimulate DnaK-mediated ATP hydrolysis at pH 4.5 (Figure 5A) is due to its low binding affinity at this pH.

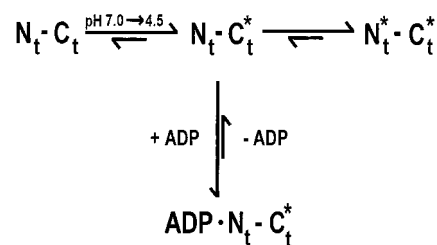


FIGURE 6: Proposed chemistry of DnaK at pH 4.5. N_t and C_t denote the ATPase and peptide-binding domains of DnaK, respectively. The asterisk denotes an altered conformation relative to pH 7.

Using the same reagent concentrations as described above, we could not detect any binding of either the fCro peptide or the fp5 peptide to ADP–DnaK at pH 4.5 (data not shown). Weak binding for three different peptides suggests a conformational change in the peptide-binding domain of DnaK; this is in accord with recent results from an NMR experiment conducted at low pH (39). In addition, when a sample of ADP–DnaK was preincubated at pH 4.5 with 10 μM fNR for 15 min, and then the pH of the sample was raised to pH 7, the amount of fNR binding to ADP–DnaK increased substantially (data not shown) and was nearly the same as for samples incubated at pH 7 (Figure 5B). The conformational change induced by the 7 to 4.5 pH jump is reversible.

The foregoing data show that incubation of DnaK at pH 4.5 affects the conformations of both functional domains. We propose that upon shifting the pH from 7 to 4.5 nucleotide-free DnaK equilibrates between two states ($N_t \cdot C_t \rightleftharpoons N_t \cdot C_t^*$) according to the model in Figure 6. N_t and N_t^* represent the ATPase domain with intact and disrupted intramolecular tertiary structure, respectively. The C-terminal domain with altered conformation is denoted by C_t^* . Nucleotide binds to the conformation with intact tertiary structure in the ATPase domain, and this binding shifts the equilibria to the nucleotide-bound state, effectively eliminating the population of molecules with a disrupted ATPase domain. Upon elimination of these conformers, tryptophan fluorescence returns to its normal level, and dye binding is significantly reduced. The $N_t \cdot C_t^*$ conformation mediates ATP hydrolysis at pH 4.5 but weakly binds added peptide. We suggest that upon a shift to pH 4 the concentration of the $N_t \cdot C_t^*$ state goes to zero; therefore, the protein is poised in the $N_t^* \cdot C_t^*$ state. Nucleotide binds weakly or not at all to this conformation, and thus no DnaK-mediated ATP hydrolysis occurs. Alternatively, we cannot rule out that nucleotide binds directly to the conformation with perturbed tertiary structure in the ATPase domain and that this binding promotes the reestablishment of tertiary structure.

This model was tested by performing limited proteolysis of DnaK in the presence and absence of nucleotide. If this model is correct, we predict that (i) the digestion pattern of DnaK should be sensitive to the presence of nucleotide at pH 4.5; (ii) preferential digestion of the ATPase domain of nucleotide-free DnaK should occur at pH 4.5; and (iii) the digestion pattern of DnaK should be relatively insensitive to the presence of nucleotide at pH 4.0. Proteolysis assays have been used at pH 7 to assess nucleotide-induced conformational changes in Hsp70 proteins (17). DnaK was subjected to limited proteolysis using cathepsin D, which is highly active between pH 3–4.5, and has a substrate specificity similar to pepsin.

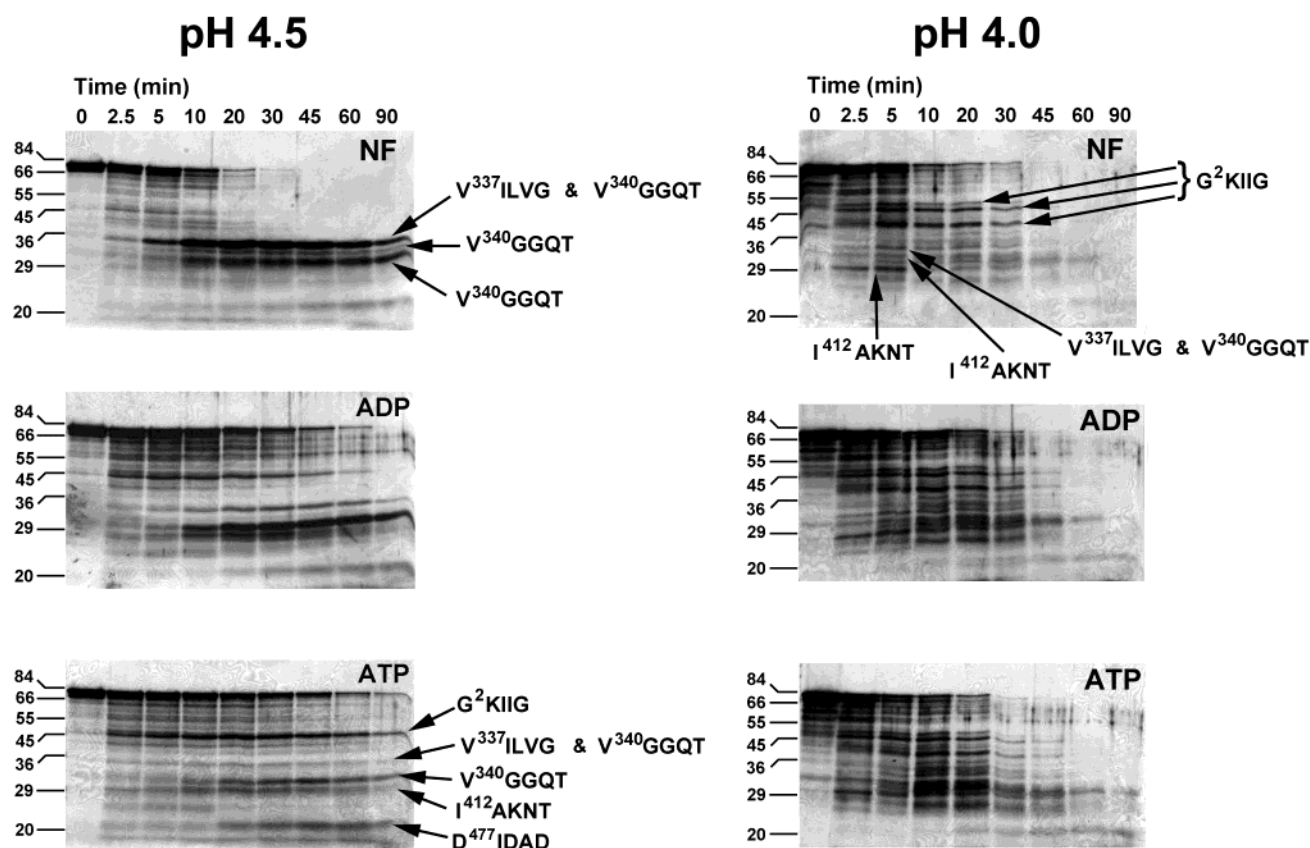


FIGURE 7: Cathepsin D digestion of DnaK. DnaK was digested by cathepsin D as described in Materials & Methods. Aliquots were removed from the reaction mixture, the reaction was halted, and the aliquots were analyzed by SDS-PAGE according to Laemmli. The left-hand panel shows digests of nucleotide-free (NF), ADP-, and ATP-bound DnaK at pH 4.5; the right-hand panel shows identical digests conducted at pH 4.0. Conditions: 10 μ M DnaK, 1 mM ADP or ATP, 0.3 units of cathepsin D; temperature = 35 $^{\circ}$ C.

Cathepsin D Digestion of DnaK. Cathepsin D digests of DnaK at pH 4.5 and 4.0 are shown in the left- and right-hand portions of Figure 7, respectively. Inspection of the gels obtained at pH 4.5 show that nucleotide-free DnaK (top left) is digested more rapidly and with a very different pattern than either ADP- (middle left) or ATP-bound (bottom left) DnaK. Inspection of the corresponding digests of DnaK at pH 4.0 show that although the staining of the lower bands in the gel of nucleotide-free DnaK are somewhat weak (top right), the overall digestion pattern for this sample is similar to the digestion patterns of ADP- (middle right) and ATP- (bottom right) DnaK. The digestion pattern of DnaK is sensitive and comparatively insensitive to nucleotide at pH 4.5 and pH 4.0, respectively. These results are in accord with the proposed model in Figure 6.

Several of the bands in the gels were excised, and the protein fragment contained therein was transferred to an Immobilon-P^{SQ} membrane. Sequence information is given next to the bands in the gels (Figure 7). Some fragments were also subjected to MALDI-TOF mass spectrometry to obtain molecular masses. Given a fragment's N-terminal amino acid. The N-terminal sequences of the major fragments are indicated in the gels in Figure 7 and schematically in Figure 8.

The major DnaK fragments identified from the cathepsin D digestion of nucleotide-free DnaK at pH 4.5 occur at 33 and 30 kDa (NF; top left, Figure 7). Sequence analysis showed that two fragments comigrate within the band at 33

kDa: one fragment begins with V³³⁷ILVG, the other with V³⁴⁰GGQT. The 30-kDa band is composed of a fragment beginning with V³⁴⁰GGQT. A minor band, sandwiched between these two intense bands, also contains a fragment commencing with V³⁴⁰GGQT. Each of these fragments contains an intact peptide-binding domain. An important finding is that the digestion of nucleotide-free DnaK yields no fragments larger than 20 kDa of the ATPase domain (Figure 8). The ATPase domain is preferentially targeted for digestion at pH 4.5.

The major DnaK fragments identified from the cathepsin D digestion of ATP-bound DnaK at pH 4.5 are summarized as follows (ATP; bottom left of Figure 7). The intense band at 45 kDa contains an N-terminal fragment that begins with the sequence G²KIIG and has a predicted C-terminal sequence of MTTL⁴¹¹. Five fragments between 36 and 22 kDa were sequenced. Each of these fragments contains the C-terminal domain of DnaK. This analysis shows that fragments of both generally intact functional domains are detected (Figure 8). Bound ATP (and ADP) protects the ATPase domain against digestion at pH 4.5.

The major DnaK fragments identified from the cathepsin D digestion of nucleotide-free DnaK at pH 4.0 are summarized as follows (NF; top right of Figure 7). Three bands falling between 36 and 55 kDa have the same N-terminal sequence (G²KIIG). Fragments beginning with V³³⁷ILVG and V³⁴⁰GGQT comigrate within the one band centered at approximately 33 kDa. Two fragments beginning with I⁴¹²AKNT occur between 29 and 32 kDa. These four

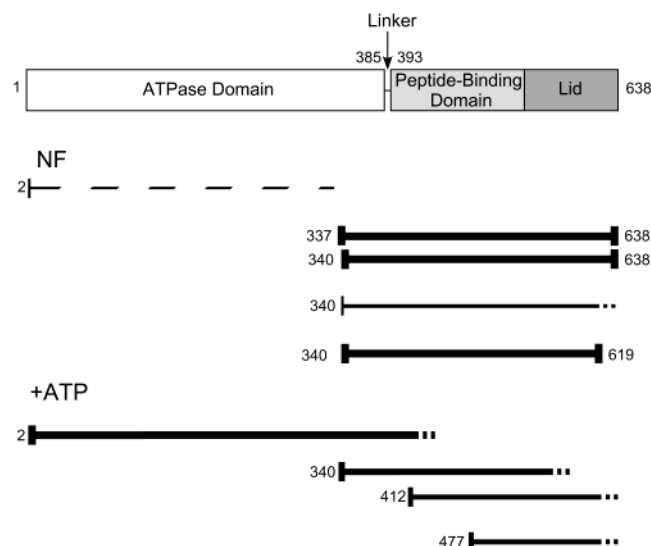


FIGURE 8: Schematic of cathepsin D digest fragments of DnaK. DnaK fragments from the digest at pH 4.5 of nucleotide-free (NF) and ATP-bound are shown. The thickness of the bar corresponds to the intensity of the fragment on the silver-stained gel. The dashed line indicates a suspected transient due to a fragment of the N-terminal domain. For three DnaK fragments, both N-terminal sequencing and mass spectral data were available, and this enabled us to predict the respective C-terminal residues. For several fragments, the reported mass is that obtained from the gels using proteins of known mass as standards. For these fragments, the respective C-terminal residue was not identified; in these cases, the C-terminal portion is denoted by dashed lines.

fragments are the peptide-binding domain of DnaK. The digestion of DnaK conducted at pH 4.0 in the absence of nucleotide yields relatively intact fragments of both functional domains. A similar digestion pattern occurs in the presence of ADP or ATP.

Kinetics of Digestion. The time course for the loss of the 70-kDa DnaK monomer band at pH 4.5 is shown in Figure 9 A. The half-times for the disappearance of the 70-kDa DnaK monomer band are 16.7, 38.0, and 51.7 min for nucleotide-free, ADP-, and ATP-bound, respectively. For comparison, the time course for the loss of the 70-kDa DnaK monomer band at pH 4.0 is shown in Figure 9B. In this case, the digestion of DnaK shows no dependence on nucleotide. The results show that there are three distinct nucleotide-dependent states at pH 4.5, whereas at pH 4 the digestion shows no appreciable dependence on nucleotide, indicating that DnaK adopts the same conformation in the absence or presence of nucleotide at this pH.

DISCUSSION

Experiments were conducted at low pH to trap and characterize stable, partially unfolded intermediates of DnaK. The spectroscopic and chemical results obtained at pH 4.5 and 4.0 are consistent with the proposed model in Figure 6. The results at pH 4.5 indicate conformational changes in both domains of DnaK. The preferential digestion of the ATPase domain at pH 4.5 could have three explanations: The domain is either unfolded, partially unfolded, or the N1 and N2 subdomains are separated. That the entire domain could be selectively unfolded is ruled out by the CD data (Figure 3B). Either partial unfolding, defined here as a decrease in tertiary structure with a retention of secondary structure, or N1 and N2 separation can explain the preferential digestion of the

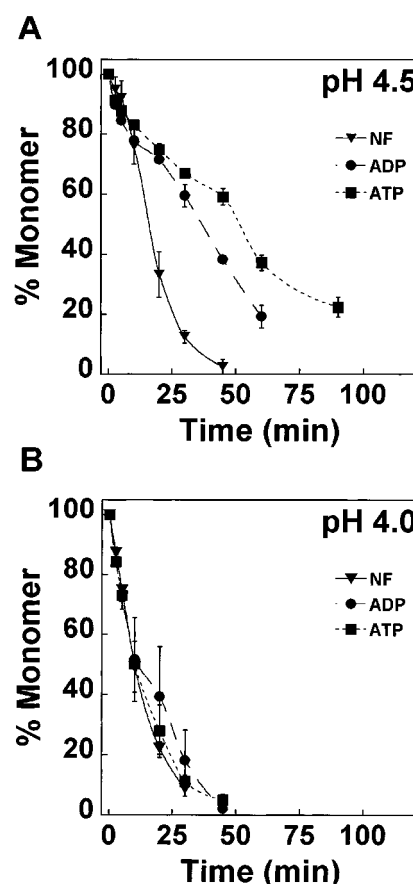


FIGURE 9: Time course for the cathepsin D digestion of DnaK. ▼, nucleotide-free; ●, ADP-bound; and ■, ATP-bound DnaK. (A) digestion at pH 4.5. (B) digestion at pH 4.0. Conditions: 10 μ M DnaK, 1 mM ADP or ATP, 0.3 units of cathepsin D, temperature = 35 °C. The fraction of the DnaK monomer ($I^m(t)/I_0^m$) was determined by scanning the gels in Figure 7 using ImageQuant software (Version 3.3, Molecular Dynamics); $I^m(t)$ and I_0^m are the integrated intensities of the DnaK monomer band at time t and time zero, respectively. NF indicates nucleotide-free DnaK.

ATPase domain at pH 4.5. Regarding the C-terminal peptide-binding domain, because of the reduced peptide binding to DnaK at pH 4.5, shifting the pH from 7 to 4.5 also produces conformational changes in the peptide-binding domain. That ATP reduces the amount of DnaK-fNR complex formation at pH 4.5 (Figure 5B) indicates that interdomain coupling may even be intact at pH 4.5.

NMR experiments on the peptide-binding site of DnaK have revealed that the lid itself occupies the substrate binding site (12). A recent NMR study of DnaK (387–522) at low pH showed that lowering the pH from 7 to 5 releases the α -helical C-terminal domain from the peptide-binding site in 10–20% of the molecules (39). Additionally, for a full-length variant of DnaK containing a tryptophan residue at position 429 (Ala429Trp), fluorescence experiments revealed that below pH 6.0 Trp⁴²⁹ shifts to a more hydrophilic environment. In light of these findings, the very weak peptide binding observed at pH 4.5 is probably a consequence of pH-induced conformational changes in the peptide-binding domain, rather than from protonation of residues in the peptide-binding site.

Compared to the findings at pH 4.5, DnaK must undergo a dramatic conformational change as the pH of the solution is lowered from pH 4.5 to 4.0. A conformational change is

not predicted by the model in Figure 6. As examples, when the pH is shifted from 4.5 to 4.0, (i) the ATPase activity of DnaK is abolished (Figure 5A); (ii) ANS binding to and the cathepsin D digestion pattern of DnaK is less sensitive to the presence of nucleotide (Figures 4 and 7); and (iii) proteolysis of DnaK occurs within 20–45 residues of the linker region (residues 385–393), yielding nearly intact functional domains. These data are interpreted to mean that the two functional domains of DnaK collapse at pH 4.0, nucleotide does not inhibit this process, and the linker region becomes more accessible to cathepsin D as compared to pH 4.5. There is an interesting parallel between this acid-induced conformational change in DnaK and a urea-denatured conformational change in the protein rhodanese: in the presence of 4.25 M urea rhodanese loses activity and intensely binds the hydrophobic dye ANS, and the protein is cleaved at the linker region between its two domains (21).

A substantial body of literature exists on the characterization of intermediates, referred to as A-states and molten globules, that form when proteins are treated with acid (for a review, see ref 37). Such work has shown that the types of conformational changes that occur depend on several factors, such as the protein, the acid, the composition of the buffer, the presence of denaturants, and the temperature. Nucleotide-free DnaK at pH 4.0 shares several features of an A-state. For example, at pH 4 nucleotide-free DnaK binds the dye ANS, has a high secondary structure content, and lacks functionality. These are some of the defining features of an A-state.

A differential scanning calorimetry study of DnaK and its two separate functional domains dissected the reversible folding behavior of DnaK (19). The lowest temperature transition (45.2 °C at pH 7.6) was assigned to the N1 cooperative folding unit. One can imagine that at the transition temperature of 45 °C, DnaK populates an intermediate in which the N1-folding unit of the ATPase domain is partially unfolded while the other 4-folding units are mainly intact. If an acidic pH jump affects the conformation of a DnaK molecule in a way similar to increasing the temperature, the conformation of nucleotide-free DnaK at pH 4.5 may be similar to the conformation of the first intermediate that occurs on heating. The preferential digestion of the ATPase domain of nucleotide-free DnaK supports this model.

ACKNOWLEDGMENT

We thank Dr. Paul Horowitz for the use of his circular dichroism instrument, Dr. Markandeswar Panda for assisting us in the CD measurements, and the staff at Olis instruments for many helpful comments and suggestions. We also thank Dr. Daniel Keppler for helpful discussions regarding the protease assay and Drs. First, Keiper, Rhoads, and Smith for a critical reading of the manuscript.

REFERENCES

1. Szabo, A., Langer, T., Schroder, H., Flanagan, J., Bukau, B., and Hartl, F.-U. (1994) *Proc. Natl. Acad. Sci. U.S.A.* 91, 10345–49.
2. Hartl, F. U. (1996) *Nature* 381, 571–580.
3. Bukau, B., and Horwich, A. L. (1998) *Cell* 92, 351–66.
4. Welch, W. J., Eggers, D. K., Hansen, W. J., and Nagata, H. (1998) *Chaperone Interactions with Nascent and Newly Synthesized Proteins*, Marcel Dekker, New York.
5. Deuerling, E., Schulze-Specking, A., Tomoyasu, T., Mogk, A., and Bukau, B. (1999) *Nature* 400, 693–6.
6. Teter, S. A., Houry, W. A., Ang, D., Tradler, T., Rockabrand, D., Fischer, G., Blum, P., Georgopoulos, C., and Hartl, F. U. (1999) *Cell* 97, 755–65.
7. Goloubinoff, P., Mogk, A., Zvi, A. P., Tomoyasu, T., and Bukau, B. (1999) *Proc. Natl. Acad. Sci. U.S.A.* 96, 13732–7.
8. Mogk, A., Tomoyasu, T., Goloubinoff, P., Rudiger, S., Roder, D., Langen, H., and Bukau, B. (1999) *EMBO J.* 18, 6934–49.
9. Diamant, S., Ben-Zvi, A. P., Bukau, B., and Goloubinoff, P. (2000) *J. Biol. Chem.* 275, 21107–13.
10. Flaherty, K. M., DeLuca-Flaherty, C., and McKay, D. B. (1990) *Nature* 346, 623–628.
11. Harrison, C. J., Hayer-Hartl, M., Di Liberto, M., Hartl, F.-U., and Kuriyan, J. (1997) *Science* 276, 431–435.
12. Wang, H., Kurochkin, A. V., Pang, Y., Hu, W., Flynn, G. C., and Zwietering, E. R. P. (1998) *Biochemistry* 37, 7929–40.
13. Zhu, X., Zhao, X., Burkholder, W. F., Gragerov, A., Ogata, C. M., Gottesman, M. E., and Hendrickson, W. A. (1996) *Science* 272, 1606–14.
14. Flynn, G. C., Chappell, T. G., and Rothman, J. E. (1989) *Science* 245, 385–90.
15. Palleros, D. R., Reid, K. L., Shi, L., Welch, W. J., and Fink, A. L. (1993) *Nature* 365, 664–6.
16. Schmid, D., Baici, A., Gehring, H., and Christen, P. (1994) *Science* 263, 971–3.
17. Buchberger, A., Theyssen, H., Schroder, H., McCarty, J. S., Virgallita, G., Milkereit, P., Reinstein, J., and Bukau, B. (1995) *J. Biol. Chem.* 270, 16903–910.
18. Palleros, D. R., Reid, K. L., McCarty, J. S., Walker, G. C., and Fink, A. L. (1992) *J. Biol. Chem.* 267, 5279–85.
19. Montgomery, D., Jordan, R., McMacken, R., and Freire, E. (1993) *J. Mol. Biol.* 232, 680–92.
20. Palleros, D. R., Shi, L., Reid, K. L., and Fink, A. L. (1993) *Biochemistry* 32, 4314–21.
21. Shibatani, T., Kramer, G., Hardesty, B., and Horowitz, P. M. (1999) *J. Biol. Chem.* 274, 33795–9.
22. Farr, C. D., Galiano, F. J., and Witt, S. N. (1995) *Biochemistry* 34, 15574–82.
23. Slepnev, S. V., and Witt, S. N. (1998) *Biochemistry* 37, 16749–56.
24. Russell, R., Jordan, R., and McMacken, R. (1998) *Biochemistry* 37, 596–607.
25. Slepnev, S. V., and Witt, S. N. (1998) *Biochemistry* 37, 1015–1024.
26. Gao, B., Greene, L., and Eisenberg, E. (1994) *Biochemistry* 33, 2048–54.
27. Gragerov, A., Zeng, L., Zhao, X., Burkholder, W., and Gottesman, M. E. (1994) *J. Mol. Biol.* 235, 848–54.
28. Gisler, S. M., Pierpaoli, E. V., and Christen, P. (1998) *J. Mol. Biol.* 279, 833–40.
29. Buczynski, G., Slepnev, S. V., Sehorn, M. G., and Witt, S. N. (2001) *J. Biol. Chem.* 276, 27231–6.
30. Lakowicz, J. R. (1999) *Principles of Fluorescence Spectroscopy*, 2nd ed., Kluwer Academic/Plenum.
31. Adler, A. J., Greenfield, N. J., and Fasman, G. D. (1973) *Methods Enzymol.* 27, 675–735.
32. Laemmli, U. K. (1970) *Nature* 227, 680–5.
33. Morrissey, J. H. (1981) *Anal. Biochem.* 117, 307–10.
34. Dawson, R. M. C., Elliot, D. C., Elliot, W. H., and Jones, K. M. (1986) *Data for Biochemical Research*, 3rd ed., Oxford Science Publications.
35. Tycho, R., and Dabagh, G. (1990) *Chem. Phys. Lett.* 173, 461.
36. Theyssen, H., Schuster, H.-P., Packschies, L., Bukau, B., and Reinstein, J. (1996) *J. Mol. Biol.* 263, 657–70.
37. Fink, A. L. (1995) in *Annual Review of Biophysics and Biomolecular Structure*, pp 495–522, Annual Reviews, Palo Alto, CA.
38. Semisotnov, G. V., Rodionova, N. A., Razgulyaev, O. I., Uversky, V. N., Gripas, A. F., and Gilmanshin, R. I. (1991) *Biopolymers* 31, 119–28.
39. Swain, J. F., Sivendran, R., and Gierasch, L. M. (2001) *Biochem. Soc. Symp.*, 69–82.